Image Orientation by Combined (A)AT with GPS and IMU

Helge Wegmann

Institute for Photogrammetry and GeoInformation, University of Hannover,
Nienburger Str. 1, 30167 Hannover, Germany
wegmann@ipi.uni-hannover.de

KEY WORDS: GPS, IMU, Direct Sensor Orientation, Integrated Sensor Orientation

During recent years the direct sensor orientation with GPS and IMU has gained popularity. These systems allow the determination of all exterior orientation elements without using ground control points. This technology opens several new applications for photogrammetry and remote sensing.

One precondition for direct sensor orientation with GPS and IMU is the correct sensor calibration. The related parameters as well as the relation between the IMU and the aerial camera (boresight misalignment) have to be determined by conventional bundle block adjustment. During this process a camera self calibration (focal length, principal point, additional parameters etc.) may be performed under operational conditions. To achieve the full accuracy potential of direct sensor orientation, the compensation of systematic errors with the correct mathematical model and an optimum number of parameters for sensor calibration is required. A series of tests was conducted and showed the good accuracy potential of direct GPS/IMU sensor orientation. First investigations showed also problems with y-parallaxes of stereo models based on direct sensor orientation.
Future developments in GPS and IMU sensors and data processing may reduce this problem. Just now we do need another save solution. A promising one is the integration of GPS/IMU and (automatic) aerial triangulation (AAT) into bundle block adjustment, also called integrated sensor orientation.
This paper presents the sensor calibration based on data from test flights in large image scales. Furthermore it demonstrates the accuracy potential at independent check points in object and in image space for direct and integrated sensor orientation.

1 Introduction

Real time mapping, for example the availability of orthoimages immediately after landing of the airplane, is a great challenge for photogrammetry. Important for achieving this aim are the newly developed digital airborne cameras Z/I-Imagine DMC (Hinz et al. 2001) and LH ADS40 (Fricker 2001). However, real time mapping cannot be realised without direct determination of the elements of exterior orientation. Therefore the elimination of ground control points in the solution was necessary. During recent years a combination of GPS and INS (Inertial Navigation System) has gained popularity, consisting of an inertial measurement unit (IMU) device and a positioning and guidance function. These systems were built for military applications and do allow the determination of all elements of exterior orientation parameters without ground control points.
A precondition for image orientation by GPS and IMU is a precise sensor calibration. The related parameter as well as the relation between the IMU and the aerial camera (boresight misalignment) have to be determined by conventional bundle block adjustment or integrated sensor orientation. During this process a camera self calibration (focal length, principal point, additional parameters etc.) may be performed under operational conditions. To achieve the full accuracy potential of direct sensor orientation and to compensate the systematic errors, a correct mathematical model with an optimum number of parameters for sensor calibration must be found.

2 Sensor Orientation with AT and GPS/IMU

The high data rate (until 200 Hz) and short time accuracy of the IMU position and attitude determination can be combined with the long-time accuracy of the GPS positions. The IMU can be used for cycle slip and multi-path detection, too. Table 1 shows the advantages of GPS/IMU integration (Skaloud 1999).

• high position and velocity accuracy
• precise attitude determination
• high data rate
• navigational output during GPS signal outages
• cycle slip detection and correction

Table 1: Benefits of GPS/IMU integration (by Skaloud 1999)

The integration of GPS and the inertial measurement system has been strongly promoted at the University of Calgary in the eighties (Schwarz et al. 1984) and a series of tests and pilot projects has been conducted demonstrating the potential of the new technology (e.g Skaloud and Schwarz 1998, Burman 1999, Cramer 1999, Heipke et al. 2002a). The same technology is also used to determine the orientation of sensors like laser scanners (Burman 2000) or SAR (Dowman 1995) sensors. Therefore the expression image orientations based on GPS and IMU can now be replaced by the more general term sensor orientation.
The sensor orientation with (A)AT and GPS/IMU consists of two steps - the GPS/IMU pre-processing and the pre-determined sensor calibration. GPS/IMU pre-processing includes the transformation of the raw GPS signal and IMU measurements into object space coordinates for the camera projection centres and roll, pitch and yaw values for each camera exposure instant. The common method of integrating GPS and IMU observations is via Kalman filtering. It provides the optimum estimation of the system based on all past and present information (for details see Skaloud 1999).

3 Mathematical Model

For the reconstruction of the 3D position and the shape of objects from images the image orientation must be known. Traditionally this task has been solved successfully by aerial triangulation. The mathematical model in bundle block adjustment is based on the well known colinearity equations.

$$\begin{aligned} x' + v_{x'} &= (x'_o + d_{x'_o}) - (f + d_f) * \frac{r_{11}(X - Xo) + r_{21}(Y - Yo) + r_{31}(Z - Zo)}{r_{13}(X - Xo) + r_{23}(Y - Yo) + r_{33}(Z - Zo)} + dx' \\ y' + v_{y'} &= (y'_o + d_{y'_o}) - (f + d_f) * \frac{r_{12}(X - Xo) + r_{22}(Y - Yo) + r_{32}(Z - Zo)}{r_{13}(X - Xo) + r_{23}(Y - Yo) + r_{33}(Z - Zo)} + dy' \end{aligned} \quad (1)$$

where

x', y, $v_{x'}$, $v_{y'}$ = image coordinates and related residuals

X,Y,Z = object coordinates in (orthogonal) ground coordinate system

Exterior Orientation:

Xo,Yo,Zo = position of projection centre in ground coordinate system

r_{ik} = elements of rotation matrix $R(\omega,\varphi,\kappa)$ between the image coordinate system an the ground coordinate system

Interior Orientation:

x'_o, y'_o = image coordinates of the principal point

dx'_o,dy'_o = corrections of the principal point

f = calibrated focal length

df = correction of the focal length

dx',dy' = effect of additional parameters

The aim of aerial triangulation is twofold, namely to determine the parameters of exterior orientation (and additional parameters by self calibration) of a block of images and simultaneously the object coordinates of the ground points (tie-, check and control points). In the case of a classical photo flight (e.g. control points are approximately in the same height level) it is not possible to separate the flying height from the correction of the focal length or the correction of the principal point from the position of projection centre. Therefore, the parameters of interior orientation (calibrated focal length, image coordinates of principal point) are, of course, needed but are assumed to be constant and known by camera calibration certificate.

This traditional method of manual aerial triangulation is time consuming (mainly the tie point extraction) and needs a sufficient number of ground control points. Today, a number of automatic aerial triangulation (AAT) software systems are commercially available as stand-alone programmes or as components of Digital Photogrammetric Workstations. With automatic aerial triangulation, the human operator only has to measure the image coordinates of ground control points, the determination of image coordinates of tie points and the computing the orientation parameters is done automatically. A series of tests was conducted and showed the good accuracy potential of AAT (Heipke and Eder 1998). Under favourable conditions (open, flat terrain and good texture) the accuracy of tie point image coordinates can be in the range of 0.15 – 0.2 pixels. Limitations of AAT show up in mountainous areas, forest and water. The accuracy of (A)AT also depends on the number and distribution of the available ground control points (GCP's) and the geometric stability of the photogrammetric block (forward and side overlap) or the quality of the direct observations for the exterior orientation parameters as observation data for the procession of the AAT.

Over the years, a number of additional sensors were used to determine at least some exterior orientation parameters directly albeit with little success until the advent of GPS (Global Positioning System) in the eighties (the system became fully operational in 1993). Using the projection centres determined by relative kinematic GPS-positioning as additional observation in the bundle adjustment a geometrically stable block based on tie points alone can be formed, and ground control information is essentially only necessary for calibration, for datum transformations, for redundancy and for detecting and eliminating the effect of GPS errors (e.g. caused by cycle slips). The functional model of GPS-supported aerial triangulation is extended by additional parameters to model systematic offsets and linear drifts of position observation, sometimes called the "shift and drift approach" (Ackermann 1994) and a GPS/aerial triangulation combination.

The GPS strip dependent additional shift and drift correction take care of remaining systematic errors in the position of the projection centres determined by GPS. This additional GPS-sensor alone does not solve all problems of direct sensor orientation, especially for single flight strips. The frequency of data registration is currently limited to 2 Hz, and GPS determines only the position. Non-traditional sensors like laser scanner systems, imaging multi-line push broom scanners and SAR sensors requires the direct determination of all elements of the exterior orientation. The GPS/IMU combination allow direct determination of all elements of exterior orientations parameters.

Inertial navigation in strap-down configuration the IMU measured in a fixed body frame system. Besides the correction due to gravity and other effects the observation have to be transformed prior to its integration into a navigation system. The definition of navigation angles are (according to ARINC 705 2000).

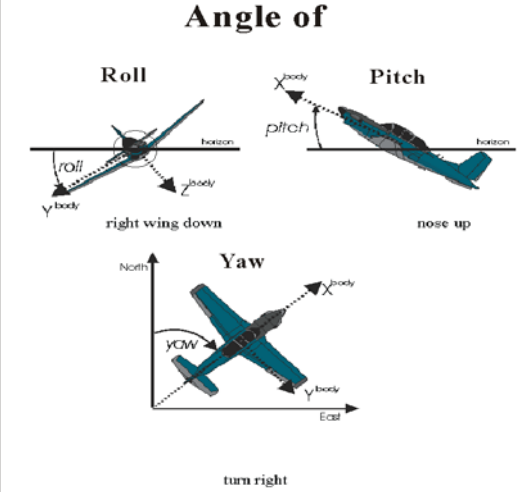

Figure 1: Definition of roll, pitch and Yaw conform to ARINC 705

The roll, pitch and yaw angles are used to transform a vector from the body coordinate system into the navigation system or from navigation into the body system (for the relation between the body coordinate system and the image coordinate system used in photogrammetry see Bäumker and Heimes 2002).

The GPS antenna and the IMU system are physically displaces from the projection centre of the camera, a constant displacement vector and a constant misalignment exist between the camera and the GPS/IMU observation. The displacement vector were measured by using conventional surveying techniques before the flight mission and is used as a lever arm correction. The body axis of the IMU cannot be physically measured. The boresight misalignment was determined during the flight by means of the first attitude reference and subtracted form the IMU attitude. The remaining differences were considered as the unknowns in the model of GPS/IMU-supported aerial triangulation.

The extended functional model
for image coordinates are (see also formula (1)):

$$\mathbf{(2)} \quad \begin{aligned} x' + v_{x'} &= f(X,Y,Z,Xo,Yo,Zo,\varpi,\varphi,\kappa,x'_o,d_{x'_o},f,d_f,dx') \\ y' + v_{y'} &= f(X,Y,Z,Xo,Yo,Zo,\varpi,\varphi,\kappa,x'_o,d_{x'_o},f,d_f,dx') \end{aligned}$$

for GPS/IMU position are:

$$\textbf{(3)}\qquad \begin{pmatrix} X_{IMU} \\ Y_{IMU} \\ Z_{IMU} \end{pmatrix} + \begin{pmatrix} v_{X_{IMU}} \\ v_{Y_{IMU}} \\ v_{Z_{IMU}} \end{pmatrix} = \begin{pmatrix} X_O \\ Y_O \\ Z_O \end{pmatrix} + R^m_c(\omega,\varphi,\kappa) \begin{pmatrix} dx^{IMU}_{Camera} \\ dy^{IMU}_{Camera} \\ dz^{IMU}_{Camera} \end{pmatrix}$$

and for GPS/IMU attitude are:

$$\textbf{(4)}\qquad \begin{pmatrix} roll^m_{b\,j} \\ pitch^m_{b\,j} \\ yaw^m_{b\,j} \end{pmatrix} + \begin{pmatrix} v_{roll,j} \\ v_{pitch,j} \\ v_{yaw,j} \end{pmatrix} = T\,[\,D\{R^m_e(\omega_j,\varphi_j,\kappa_j)\}\,(R^b_c(\text{droll},\text{dpitch},\text{dyaw}))^{-1}\,]$$

where

$x', y, v_{x'}, v_{y'}$ = image coordinates and related residuals

$X,Y,Z_{(IMU)}$
$v_X, v_Y, v_{Z(IMU)}$ = Object space coordinates of IMU centre of mass and related residuals

$roll, pitch, yaw^m_b$
$v_{roll}, v_{pitch}, v_{yaw}$ = Elements of rotation matrix between body-frame and ground coordinate system and related residuals

X,Y,Z = object space coordinates
Xo,Yo,Zo = position of projection centre in ground coordinate system
ω,φ,κ = attitude of projection centre in ground coordinate system
x'_o, y'_o = image coordinates of the principal point
dx'_o, dy'_o = corrections of the principal point
f = calibrated focal length
df = correction of the focal length
dx',dy' = effect of additional parameters
$R^m_c(\omega, \varphi, \kappa)$ = rotation matrix between the camera frame an the ground coordinate system
D = Rotation matrix to take care of the transformation form (ω,φ,κ) into (roll, pitch, yaw)
T = Transformation for extracting individual angles out of the rotation matrix
$dx, dy, dz^{IMU}_{Camera}$ = Components of offset vectors between IMU centre and projection centre, image coordinate system
$d_{roll}, d_{pitch}, dy_{aw}$ = Angles of boresight misalignment
$R^b_c(d_{roll}, d_{pitch}, d_{yaw})$ = Rotation matrix camera-frame => body frame; matrix of boresight misalignment

The GPS and IMU supported aerial triangulation is formulated corresponding to the aerial triangulation with GPS observations, i.e. as direct measurements of the attitudes with optional shift and time dependent drift parameters. Therefore, the GPS/IMU model is modified with following equation:

$$\textbf{(5)}\qquad \begin{aligned} Xo &= Xo + dXo_{Shift} + (t-to)*bXo_{drift} & \varpi &= \varpi + d\varpi_{shift} + (t-to)*b\varpi_{drift} \\ Yo &= Yo + dYo_{Shift} + (t-to)*bYo_{drift} & \varphi &= \varphi + d\varphi_{shift} + (t-to)*b\varphi_{drift} \\ Zo &= Zo + dZo_{Shift} + (t-to)*bZo_{drift} & \kappa &= \kappa + d\kappa_{shift} + (t-to)*b\kappa_{drift} \end{aligned}$$

One pre-condition for sensor orientation with aerial triangulation and GPS and IMU is the pre-determined sensor calibration. During this process a camera self calibration (focal length, principal point, additional parameters etc.) may be performed under operational conditions.

4 Test Data description

In order to analyse the mathematical model with an optimum number of parameters for sensor calibration the suitable test data "Fredrikstad", the have already been used in the OEEPE test "Integrated Sensor Orienation", was selected (Heipke et al. 2002b, Nilsen 2002, Heipke et al. 2002a).
The test data have been acquired on October 7, 1999 over the test field Fredrikstad, in Norway near the capital Oslo. The test field is maintained by the Agricultural University of Norway, Department of Mapping Sciences (IKF). The test field size is approximately 5 x 6 km² with 51 well distributed signalised ground control points known with an accuracy better than 1cm for all components. The ground control point targets have a size of 40 x 40 cm² sufficient for the image scale 1:5000 and 1:10000. During photogrammetric data acquisition several GPS receivers were in use. In order to eliminate influences of long GPS base lines, it was decided to use the stationary receiver directly in the test field as reference station.
The GPS/IMU equipment POS/AV 510-DG (Applanix of Toronto, Canada) consists of a dual frequency GPS receiver using differential carrier phase measurements and a high quality off-the-shelf navigation grade IMU as typically used in precise airborne position and attitude determination. The test flights were carried out by the Norwegian companies Fotonor AS. Fotonor used an Ashtech GPS receiver and the Applanix POS/DG AIMU equipment tightly coupled to a wide angle Leica RC30, the latter mounted on the gyro-stabilised platform PAV30. The PAV30 data and thus rotations of the camera and the IMU relative to the plane body were recorded and introduced into further processing. The system included a Litton LN-200 IMU. The LN-200 uses fibre optic gyros and silicon accelerometers for the measurement of vehicle angular rate and linear acceleration. The claimed accuracy is for the positions better than 0.1 m, in roll, pitch better than 0.005 degree and in yaw better than 0.008 degree.

Camera		Leica RC 30, c = 153 mm
GPS receiver (aircraft)		Ashtech Z Surveyor (L1,L2)
data rate		0.5 sec.
IMU		Littion Ln-200
data rate		200 Hz
GPS/IMU system		Pos / AV 510-DG
claimed accuracies	position	< 0.1m
	roll, pitch	< 0.005 deg.
	yaw	< 0.008 deg.

Table 2: Applanix data acquisition equipment

The aircraft was flown at an altitude of 800 and 1600 meters above ground resulting in an image scale of 1:5000 and 1:10000, respectively. In order to achieve a good initial alignment for the IMU axes with the gravity field, the aircraft made an S-like turn before the first flight strip.
The first 1:5000 flight, called also calibration flight, consist of two strips in east/west direction and two strips in north/south direction. Each strip was flown twice in opposite directions. The two directions are necessary for dynamic GPS/IMU alignment. The opposite flight directions are required for the separation of the GPS shift parameters and the location of the camera principal point.

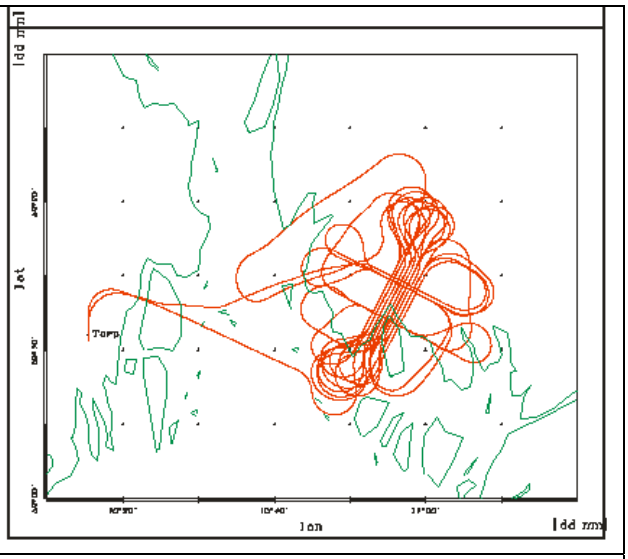

Figure 2: Flight path

The 1:10000 test flight comprises four parallel strips and one cross strip and covers the whole test field. The cross strip and one of the parallel strips were flown twice in opposite directions, too. Apart from the possibility to check the calibration parameters in another image scale the second scale is required to resolve the high correlation between the vertical GPS shift and the correction of the focal length.
Following the two calibration flights, a test flight in the scale 1:5000 covering the complete test field was carried out, see figure 3. It includes 9 parallel and 2 crossing strips. All flights were carried out with a forward and side overlap of 60 %.

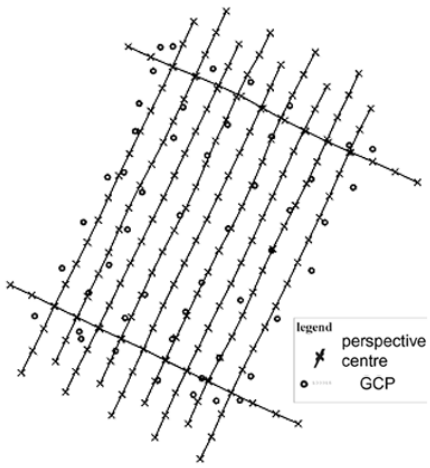

Figure 3: Test flight 1:5 000

5 Sensor Calibration and Orientation

The colinearity equations, which define the relation between the object point, image coordinates and sensor orientation are based on an orthogonal coordinate system. The earth curvature and the national coordinate systems (e.g. UTM) do not correspond to this. In traditional photogrammetric projects the effects of non orthogonal systems are sometimes compensated by an earth curvature correction applied to the image coordinates. For a combined adjustment with image coordinates and direct observations of position and attitude the usual earth curvature correction is not sufficient, a computation in a geocentric or a tangential system solves this problem (see a discussion on these effects in Jacobsen 2002). The following discussion of direct and integrated sensor calibration is based on a local tangential system.

5.1 Sensor Calibration

The sensor calibration, whether for direct or integrated sensor orientation in a combined bundle adjustment, requires image coordinates, the GPS/IMU observations and ground control information as input. It should be noted that often no stochastic information available for the GPS/IMU measurements after the Kalman filter, therefore the accuracy values for the position and attitude observation given in the data sheets of Applanix were used (table 3) in the combined bundle adjustment.
The accuracy values for the observation are:

image coordinates	= ± 6 µm
GCP	= ± 1 cm
GPS/IMU position	= ± 0.1 m
GPS/IMU roll, pitch	= ± 5.5 mgon
GPS/IMU yaw	= ± 8.9 mgon

Table 3: Stochastic model

The OEEPE Test "Integrated Sensor Orientation" has been conducted demonstrating that the number of system calibration parameters estimated in the adjustment depend on the accuracy of sensor orientation (Heipke et al. 2002a). The traditional sensor calibration with (A)AT and GPS/IMU uses the six standard parameters. The six parameters solution consists of three GPS shifts and three misalignment angles, which can be computed from only one calibration flight. The result of the system calibration estimated in a combined bundle block adjustment for the calibration flight 1:5000 and 1:10 000 and in combination of both calibration flights are:

calibration flight	**parameters**	**values**	**stand. dev.**
1: 5 000	IMU shift	Δω = 0.1041 gon Δφ = 0.0532 gon Δκ = 161.8392 gon	± 0.6 mgon ± 0.6 mgon ± 1.2 mgon
	GPS shift	dXo = 0.104 m dYo = -0.053 m dZo = 0.301 m	± 0.6 cm ± 0.7 cm ± 2.1 cm
1: 10 000	IMU shift	Δω = 0.1039 gon Δφ = 0.0548 gon Δκ = 161.8375 gon	± 0.7 mgon ± 0.7 mgon ± 1.4 mgon
	GPS shift	dXo = 0.124 m dYo = -0.063 m dZo = 0.521 m	± 1.2 cm ± 0.8 cm ± 3.5 cm
1: 5000 + 1: 10000	IMU shift	Δω = 0.1032 gon Δφ = 0.0561 gon Δκ = 161.8383 gon	± 0.6 mgon ± 0.5 mgon ± 1.2 mgon
	GPS shift	dXo = 0.119 m dYo = -0.058 m dZo = 0.401 m	± 0.6 cm ± 0.5 cm ± 2.8 cm

Table 4: Sensor calibration values with six parameters

The attitude differences between the IMU and the image coordinate systems (misalignment) are independent of image scale and are more or less stable. Therefore, these parameters

can be used as sensor calibration parameters. On the other hand, the GPS shift parameters depend on image scale. Therefore, additional calibration parameters are required for modelling the remaining systematic effects.
The focal length and the position of principle point values of the camera certificate is calibrated in a laboratory e.g. under constant temperature condition. During photo flight there are not the same condition like in the laboratory (Jacobsen and Wegmann 2002). Thus, the values of the calibration certificate cannot be used for the direct sensor orientation, when the calibration flight has a different altitude than the project flight. The calibration parameters for direct sensor orientation should include the six standard calibration parameters and also the interior orientation performed under flight condition.
The parameters of interior orientation can be determined together with the other elements of the boresight misalignment, when a calibration flight is done in different height levels and two strips in opposite flight direction. The calibration of the interior orientation nine parameter solution its quite possible with the combination of the calibration flight 1:5000 and 1:10000. The results are:

parameters	values	stand. dev.
IMU shift	$\Delta\omega$ = 0.1032 gon $\Delta\varphi$ = 0.0561 gon $\Delta\kappa$ = 161.8383 gon	± 0.6 mgon ± 0.5 mgon ± 1.2 mgon
GPS shift	dXo = 0.108 m dYo = -0.033 m dZo = 0.091 m	± 0.6 cm ± 0.5 cm ± 2.4 cm
Interior Orientation	dx'_o = -7.1 µm dy'_o = 65.6 µm df = -6.8 µm	± 1.1 µm ± 0.9 µm ± 2.9 µm

Table 5: Calibration values with nine parameters

For the interpretation of the results, it should not be forgotten, however, that a refinement of the interior orientation parameters during the calibration does not necessarily mean that the camera calibration certificate contains incorrect values. It only implies, that the more general models better explain the given input data. For instance, a change in the principal point (in flight direction, see dy'_o in table 5) has nearly the same effect on the results as a constant error in the time synchronisation between the GPS/IMU sensors and the camera. The same is true for a change in the calibrated focal length and the GPS shift in Z.

5.2 Direct Sensor Orientation

The influence of different additional parameter sets for the direct sensor orientation is illustrated with the following example from the block flight 1:5000.The measured image coordinates of 49 independent check points (ICP's) have been transformed into object space via a least-squares forward intersection with the exterior orientations of the calibrated GPS/IMU observations (six system calibration parameters from calibration flight 1:5000) as constant values. The resulting ground coordinates have been compared with the known values of the ICP's (see table 6).

No. of system calibration parameters	σ_o [µm]	RMS differences at ICP's		
		X [cm]	Y [cm]	Z [cm]
6	30.1	10.5	11.0	13.0
9	14.4	5.8	6.8	8.8

Table 6: Results for varying number of calibration parameters

The results depend on the number of parameters estimated during the system calibration. A change of the calibrated focal length and the position of the principal point improves the result significantly. The accuracy of the direct sensor orientation is in the range of 5 cm in planimetry and 9 cm in height at independent check points and at approximately 15 µm in image space.
The results presented in table 6 are based on multiple rays per point. But of course, if multiple rays are given, it is more advantageous to perform an integrated sensor orientation. A more detailed analysis of the obtainable accuracy with only two rays per point has been made. 178 individual models can be formed from the test block 1:5000. Based on these models, via least square forward intersection, object coordinates for all ICP's could be determined and were compared with the known values. The model accuracy in object space (root mean square differences at independent check points) and in image space $\sigma_{o,rel}$ (average RMS remaining y-parallaxes per model) together with the percentage of models with RMS y-parallaxes exceeding 10 and 20 µm are presented in table 7.

σ_o [µm]	$\sigma_{o,rel}$ [µm]	RMS discrepancies at ICP's			% of models with RMS y-parallaxes	
		X [cm]	Y [cm]	Z [cm]	> 10 µm	> 20µm
14.4	15.3	5.8	6.0	10.5	80	11

Table 7: Accuracy of models in object and image space

Table 7 shows that not all models based on direct sensor orientation can be used for stereo plotting. 80 % of the models have y-parallaxes exceeding 10 µm (stereo plotting becomes less comfortable) and 11% of the stereo models have y-parallaxes larger than 20 µm (stereo plotting becomes cumbersome).

5.3 Integrated Sensor Orientation

When comparing direct and integrated sensor orientation, the role of IMU data changes. In both cases the IMU data serve as input for GPS/IMU pre-processing and do increase the quality of the derived projection centre positions during image acquisition. For direct sensor orientation the IMU data are furthermore indispensable as direct observations for the roll, pitch, and yaw angles. This is not the case anymore for integrated sensor orientation of image blocks, because these angles can also be computed from the image coordinates of the tie points. To compare the results from direct and integrated sensor orientation, the block configuration (60 % side overlap) for the test block 1:5000 will not be used. The "new" test data set comprises now nine parallel strips and the tie points from the test flight 1:5000 as input. In table 8 the results of the strip adjustment are given, consisting of the a posteriori standard deviation of the image coordinates and the RMS differences of the derived object space coordinates of 49 ICPs.

No. of system cali. parameters	σ_o [µm]	RMS differences at ICPs		
		X [cm]	Y [cm]	Z [cm]
9	5.2	5.4	6.2	7.5

Table 8 : Results for integrated sensor orientation

Compared to the results based on the direct sensor orientation the additional introduction of tie points in integrated sensor orientation without GCPs improves in particular the accuracy in image space, and to some extent also in object space. As expected, integrated sensor orientation overcomes the problem

of remaining y-parallaxes in photogrammetric models and allows for the determination of 3D object space information in the same way as conventional photogrammetry.

6 Conclusion

Direct Sensor Orientation has been proven to be a serious alternative to aerial triangulation. The test resulted in RMS differences for ground points of 5 cm in planimetry and 10 cm in height at independent check points obtained with multi-ray and in similar values for two-ray points in an image scale 1:5 000. Obviously, the values for two-ray points are more relevant, because if multi-ray points are available an integrated sensor orientation can be computed. While these values are larger by a factor of 2 – 3 when compared to standard photogrammetric results, it seems to be safe to conclude that direct sensor orientation currently allows the generation of orthoimages and ground points with less stringent accuracy requirements. Stereo plotting, on the other hand, is not always possible using direct sensor orientation due to the sometimes large y-parallaxes in individual models. To overcome the problem of too large remaining y-parallaxes, the combination of GPS/IMU observations with tie points - the integrated sensor orientation - should be preferred.

Based on the obtained results, the actual determination of the interior orientation parameters in the system calibration is recommended whenever possible. If it is not feasible to use two calibration flights at significantly different flying heights, the calibration should be carried out at the same height (and thus the same scale) as the actual project.

7 References

Applanix (1999) POS/DG POS/AV 510-DG Specifications, http://www.applanix.com, Ontario, Canada

ARINC 705: http://www.arinc.com/cgi-bin/store/arinc (Accessed July-3rd-2001).

Ackermann, F., (**1994**): *On the status and accuracy performance of GPS photogrammetry* Proceedings, ASPRS Workshop "Mapping and remote sensing tools for the 21st Century, Washington D.C., USA, pp. 80-90.

Burman, Helén, (**1999**): *Using GPS and INS for orientation of aerial photography* Proceedings ISPRS Workshop "Direct versus indirect methods of sensor orientation" Barcelona, Spain, pp. 148 - 157 .

Burman, Helén, (**2000**), *Calibration and Orientation of Airborne Image and Laser Scanner Data Using GPS and INS*, Ph. D. Thesis, Photogrammetric Reports No 69Royal Institute of Technology, Stockholm, Sweden.

Bäumker, Manfred and Heimes, Franz, J., (**2002**): *New Calibration and Computing Method for Direct Georeferencing of Image and Scanner Data Using the Position and Angular Data of an Hybrid Intertial Navigation System* in: C. Heipke, K. Jacobsen and H. Wegmann (Eds.), Integrated Sensor Orientation, OEEPE Official Publcation No. 43, Bundesamt für Kartographie und Geodäsie, Frankfurt am Main, pp. 197 – 212.

Cramer, Michael, (**1999**): *Direct geocoding - is aerial triangulation obsolete ?* in: Fritsch/Spiller (Eds.), Photogrammetric Week ´99 Herbert Wichmann Verlag, Hüthig GmbH, Heidelberg, Germany, pp. 59 - 70 .

Dowman, Ian, (**1995**): *Orientation of SAR Data: Requirements and Applications* in: C. Ismael and J. Navarro (Eds.), Integrated Sensor Orientation, Herbert Wichmann Verlag, Heidelberg, Germany, pp. 156 - 165 .

Fricker, Peter, (**2001**): *ADS40 - Progress in digital aerial data collection* in: Fritsch/Spiller (Eds.), Photogrammetric Week ´01 Herbert Wichmann Verlag, Hüthig GmbH, Heidelberg, Germany, pp. 105 - 116.

Heipke, Christian and Eder, **Konrad,** (**1998**): *Performance of tie point extraction in automatic aerial triangulation* , OEEPE Official Publcation No. 35 Verlag Bundesamt für Kartographie und Geodäsie, Frankfurt am Main, Germany, pp. 127 - 185, .

Heipke, Christian, Jacobsen, Karsten and Wegmann, Helge, (**2002**): *Analysis of the results of the OEEPE test "Integrated Sensor Orientation"* in: C. Heipke, K. Jacobsen and H. Wegmann (Eds.), Integrated Sensor Orientation, OEEPE Official Publcation No. 43 Verlag Bundesamt für Kartographie und Geodäsie, Frankfurt am Main, Germany, pp. 31 - 49, . (a)

Heipke, Christian, Jacobsen, Karsten, Wegmann, Helge, Andersen, Østein and Nilsen, Barbie, Jr., (**2002**): *Test goals and test set up for the OEEPE test "Integrated Sensor Orientation"* in: C. Heipke, K. Jacobsen and H. Wegmann (Eds.), Integrated Sensor Orientation, OEEPE Official Publcation No. 43 Bundesamt für Kartographie und Geodäsie, Frankfurt am Main, Germany, pp. 11 - 29, . (b)

Hinz, Alexander, Dörstel, Christoph and Heier, Helmut, (**2001**): *DMC - The Digital Sensor Technology of Z/I-Imaging* in: Fritsch/Spiller (Eds.), Photogrammetric Week ´01 Herbert Wichmann Verlag, Hüthig GmbH, Heidelberg, Germany, pp. 93 - 103, .

Jacobsen, Karsten and Wegmann, Helge, (**2002**): *Dependencies and problems of direct sensor orientation* in: C. Heipke, K. Jacobsen and H. Wegmann (Eds.), Dependencies and problems of direct sensor orientation, OEEPE Official Publcation No. 43 Bundesamt für Kartographie und Geodäsie, Frankfurt am MainOrt Frankfurt am Main, Germany, pp. 73 - 84, .

Jacobsen, Karsten, (**2002**): *Transformations and computation of orientation data in different coordinate systems* in: C. Heipke, K. Jacobsen and H. Wegmann (Eds.), Integrated Sensor Orientation, OEEPE Official Publcation No. 43, Bundesamt für Kartographie und Geodäsie, Frankfurt am Main, Germany, pp. 179-188, .

Nilsen, Barbie, Jr., (**2002**): *Test field Frederikstad and data acquisition for the OEEPE test "Integrated Sensor Orientation"* in: C. Heipke, K. Jacobsen, H. C. Wegmann, K. Jacobsen and H. Wegmann (Eds.), Integrated Sensor Orientation, OEEPE Official Publcation No. 43 Bundesamt für Kartographie und Geodäsie, Frankfurt am Main, Germany, pp. 19 - 30, .

Schwarz, K., P., Fraser, C.,S. and Gustafson, P.,C., (**1984**): *Aerotriangulation without Ground Control* International Archives of Photogrammetry and Remote Sensing, Vol. 25, Part A1, Rio de Janeiro, Brazil,.

Skaloud, Jan and Schwarz, Klaus, P., (**1998**): *Accurate orientation for airborne mapping systems* IAPRS (32) 2 pp. 283 - 290, .

Skaloud, Jan, (**1999**), *Optimizing Georeferencing of Airborne Survey Systems by INS/DGPS*, Ph. D. Thesis, UCGE Report 20216 University of Calgary, Alberta, Canada.